IET Electric Power Applications

Research Article

Online multi-parameter estimation of interior permanent magnet motor drives with finite control set model predictive control

ISSN 1751-8660
Received on 31st July 2016
Revised on 10th November 2016
Accepted on 19th December 2016
doi: 10.1049/iet-epa.2016.0514
www.ietdl.org

Shamsuddeen Nalakath[1] ✉, *Matthias Preindl*[2], *Ali Emadi*[1]

[1]*Department of Electrical and Computer Engineering, McMaster University, Hamilton, Ontario, Canada*
[2]*Department of Electrical Engineering, Columbia University in the City of New York, New York, USA*
✉ *E-mail: nalakas@mcmaster.ca*

Abstract: This study presents an online multiparameter estimation scheme for interior permanent magnet motor drives that exploits the switching ripple of finite control set (FCS) model predictive control (MPC). The combinations consist of two, three, and four parameters are analysed for observability at different operating states. Most of the combinations are rank deficient without persistent excitation (PE) of the system, e.g. by signal injection. This study shows that high frequency current ripples by MPC with FCS are sufficient to create PE in the system. This study also analyses parameter coupling in estimation that results in wrong convergence and propose a decoupling technique. The observability conditions for all the combinations are experimentally validated. Finally, a full parameter estimation along with the decoupling technique is tested at different operating conditions.

1 Introduction

The drive systems especially used in high performance applications are getting smaller and lighter [1]. These benefits are usually traded with operating the electric machines at their boundaries where the machine parameters vary significantly. The parameters which undergo variations are broadly classified as mechanical, thermal and electrical. This paper focuses on estimation of electrical parameters of interior permanent magnet (IPM) machines viz., stator phase resistance (R_s), d- and q-axis inductances (L_d and L_q), and permanent magnet flux linkage (ψ_m). The stator resistance varies with temperature and operating frequency, whereas permanent magnet flux linkage changes with temperature and demagnetisation. The inductances vary with saturation of electromagnetic core. The parameter variations influence the operation and stability of the control system especially if a model-based control is used. The online estimation techniques can be used to track the parameters. However, the system needs to be observable with respect to the estimating parameters.

The machine model is generally treated as linear by assuming constant speed and machine parameters. Thereby, it allows the application of classical linear observability theory to verify the system observability [2, 3]. The machine can also be modelled as a linearly varying parameter model. The persistent excitation (PE) condition is chosen as the observability condition for this case [4, 5]. However, the lack of information about which input needs to be persistently excited is the main limitation [6]. Another approach is linearising the machine model in a certain state subspace in order to apply the linear observability theorem [7, 8]. This approach is very localised and lacks the sense of observability in the entirety of the state trajectories. The analysis of global observability of the non-linear dynamic system is difficult in practice [9]. The construction of a global observer which converges every trajectory is impossible as the non-linear system attempts many singular cases on the go. The local observability is a powerful concept which can be applied to any non-linear systems [10]. The concept distinguishes states only from their neighbours. The theory proposed by Hermann and Kerner with the help of Lie-theoretic characterisation is one of the most widely used methods [11]. The theory shows that the rank criteria are sufficient to verify the local observability of a non-linear system.

The estimation of one parameter is always observable as long as the operating states meet the required conditions. For example, the condition $\omega \neq 0$ for estimating ψ_m. On the other hand, the observability of simultaneous estimation of two or more parameters depends on the combination in addition to the operating states [12]. The non-linear observability analysis of electric machines available in the literature is mainly based on the concept proposed by Hermann Kerner [12–14]. The observability analysis used to estimate parameter combinations without PE for a permanent magnet machine is presented in [12]. It is shown that the estimation of R_s and L_s is always possible as long as speed and i_q are non-zero. The observability conditions for estimating speed, position and resistance for induction motor (IM) and permanent magnet synchronous motor (PMSM) are presented in [13], while the observability conditions to estimate position for surface permanent magnet (SPM) and IPM are analysed in [14]. It is shown that IPM is always observable in contrast to SPM. As there is an opportunity for IPM to make the system rank sufficient even at zero speed by persistent current injection. The literature available so far analyses the observability of a few parameter combinations but a detailed analysis covering all the possible combinations is lacking.

Not all the parameters are observable for IPMs at steady state [12, 15]. This problem can be overcome by injecting high frequency signals. The full parameter estimation, achieved by injecting sine and square wave signals at the d-axis is, compared in [15] and it is shown that the sine wave injection has faster convergence. The robustness of the estimation of all the parameters with signal injection is improved by decoupling slow and fast parameters with two differently sampled recursive least square (RLS) estimators [16]. The slow parameters from the high frequency model and the fast parameters by RLS are estimated [17]. A complete decoupling is achieved in this case by the fact that the two estimators are based on different models (high frequency and fundamental). In [18], two affine projection estimators are used for slow and fast parameters. The full parameter estimation is fairly established in the literature besides the fact that some of the details are not well addressed. This includes the possible higher discretisation error due to lower sampling rate associated with slow parameter estimation and the parameter dependencies. The dependency between R_s and ψ_m is mentioned in [19], however a detailed analysis and compensation techniques are not presented.

This paper focuses on detailed observability analysis of all the possible combinations consisting of two, three and four parameters. The observability at worst-case scenarios such as steady state, $i_d = 0$, and $\omega = 0$ are analysed and the scenarios which require PE are identified. The current ripple due to inherent high frequency vector injection of model predictive control with finite control set (MPC-FCS) is considered in this paper as PE [20, 21]. This paper also shows that parameter coupling between R_s and ψ_m is significant for the reference IPM machine. This phenomenon is analysed and a compensation technique is proposed. The RLS is chosen as the estimator in this paper. The observability of different combinations of the parameters is validated experimentally. The full parameter estimation with decoupling technique is tested for different operating points. This paper is organised as Section 2 covers the theoretical observability analysis and Section 3 presents estimation scheme and experimental setup. Section 4 presents the experimental results and discussions, and the conclusion of the paper is provided in Section 5.

2 Observability analysis

The local observability concept proposed by Hermann and Kerner for non-linear dynamic systems is briefly discussed as follows [7]: If a system Σ is locally observable at initial state x_0, then in every open neighbourhood U of x_0 is distinguishable

$$I_U(x_0) = \{x_0\} \tag{1}$$

and therefore Σ is locally observable at every $\boldsymbol{x} \in M$ (M is universal set). The system Σ is locally weakly observable if there exists a neighbourhood V of x_0 which is contained in the open neighbourhood U in such a way that

$$I_V(x_0) = \{x_0\} \tag{2}$$

and for every $\boldsymbol{x} \in M$. The benefit of local weak observability is that it can be verified by a simple algebraic test [7]. The test is based on the rank of $\boldsymbol{O}$, Jacobian of the Lie derivative vector

$$\boldsymbol{O} = \frac{\partial}{\partial \boldsymbol{x}} \begin{pmatrix} L_f^0 h \\ L_f^1 h \\ \cdots \\ L_f^{(n-1)} h \end{pmatrix} \tag{3}$$

where $L_f^{(n-1)}h$ is the Lie derivative of output vector $\boldsymbol{h}$ with respect to system function f, and n is the dimension of state vector $\boldsymbol{x}$. The size of $\boldsymbol{O}$ is the size of $\boldsymbol{h}$ multiplied by $(n-1)$ times n. If the rank of $\boldsymbol{O}$ is n, then the system is fully observable (locally weakly). It is laborious to analyse the rank of a large matrix like $\boldsymbol{O}$ at different states. The general practice is to choose a proper sub matrix [12–14].

2.1 IPM observability

The parameters vary in different degrees in an electric machine. However, a slow variation is assumed for all the parameters in this paper for the sake of simplicity in the mathematical formulation. It is to be noted that, if a slow variation is observable, then it is most likely observable for fast variation. The system of equations of an IPM machine by considering slow parameter variations and constant angular speed is given in (4) [12]. All four of the parameters, consisting of d- and q-axis inductances (L_d and L_q), phase resistance (R_s) and permanent magnet flux linkage (ψ_m), are considered varying in (4). The mutual inductances are not explicitly modelled in this paper. However, its effect can be observed from self-inductance as presented in the result section of this paper

$$\begin{aligned} \frac{\mathrm{d}i_d}{\mathrm{d}t} &= -\frac{R_s}{L_d} i_d + \omega \frac{L_q}{L_d} i_q + \frac{1}{L_d} v_d \\ \frac{\mathrm{d}i_q}{\mathrm{d}t} &= -\frac{R_s}{L_q} i_q - \omega \frac{L_d}{L_q} i_d - \omega\psi_m + \frac{1}{L_q} v_q \\ \frac{\mathrm{d}L_d}{\mathrm{d}t} &\cong 0 \\ \frac{\mathrm{d}L_q}{\mathrm{d}t} &\cong 0 \\ \frac{\mathrm{d}R_s}{\mathrm{d}t} &\cong 0 \\ \frac{\mathrm{d}\psi_m}{\mathrm{d}t} &\cong 0 \end{aligned} \tag{4}$$

To analyse the observability of the above non-linear system, the local observability theorem needs to be applied. The first step is finding the Jacobian matrix $\boldsymbol{O}$ given in (3). The system function (4) represents f in (3). The state vector, $\boldsymbol{x}$, is $[i_d\ i_q\ L_d\ L_q\ R_s\ \psi_m]$. The output vector, $\boldsymbol{h}$, is $[i_d\ i_q]$. A detailed formulation of the Lie derivatives and Jacobian matrix for estimation of electric machine parameters is given in [13, 14].

This paper analyses non-linear observability for different combinations of the parameters. The parameter combinations are categorised into groups of two, three or four parameters. It should be noted that all the four parameters are varying in (4). However, for a combination, only the associated parameters are considered varying and rest of them are assumed as constants.

Combination 1 only considers variation in L_d and L_q while assuming R_s and ψ_m as constants and therefore the state vector is, $\boldsymbol{x} = [i_d\ i_q\ L_d\ L_q]$. The output vector ($\boldsymbol{h}$) remains the same as the system (4) and will be the same for all other combinations. The Jacobain for this case is a 6×4 matrix as given below: (see (5))

$$\boldsymbol{O}_1 = \begin{bmatrix} 1 & 0 & 0 & 0 \\ 0 & 1 & 0 & 0 \\ -R_s & \omega L_q & -\dfrac{\mathrm{d}id}{\mathrm{d}t} & \omega i_q \\ -\omega L_d & -R_s & -\omega i_d & -\dfrac{\mathrm{d}iq}{\mathrm{d}t} \\ -R_s^2 - (\omega L_d)^2 & -R_s\omega(L_d + L_q) & -2\dfrac{d^2 id}{\mathrm{d}t^2} L_d + \omega\left(L_q \dfrac{\mathrm{d}iq}{\mathrm{d}t} - i_d L_d \omega\right) & i_q R_s \omega \\ R_s\omega(L_d + L_q) & R_s^2 - (\omega L_q)^2 & i_d R_s \omega & -2\dfrac{d^2 iq}{\mathrm{d}t^2} L_q + \omega\left(-L_d \dfrac{\mathrm{d}id}{\mathrm{d}t} - L_q i_q \omega\right) \end{bmatrix} \tag{5}$$

The rows from top to bottom correspond to derivatives of output vector from zero to second orders, respectively. The columns from left to right represent the variations in i_d, i_q, L_d and L_q, respectively. The rank requirement for the system to be fully observable is four. However, as i_d and i_q are measurements and always observable, the columns corresponding to i_d and i_q can be eliminated from $\boldsymbol{O}_1$. Hence the rank requirement for the system to observe all the parameters (L_d and L_q) becomes just two (number of the estimating parameters). One of the proper sub matrices which has the columns corresponding to variations in only L_d and L_q with rank two is (see equation (6) at the bottom of he next page)

According to the rank of $\boldsymbol{O}_{s1}$, L_d and L_q can be estimated simultaneously at steady state and even at $\omega = 0$. If $i_d = 0$ only L_q can be estimated. However, it can be estimated even if the average $i_d = 0$ while the derivative of i_d is not equal to zero. Similarly with i_q for the case of L_q. This means that with a PE both the parameters can be estimated even when the average values of the associated currents are zero which is a case in MPC-FCS.

The proper sub matrix of Jacobian matrix considering the variations in only R_s and ψ_m, where L_d and L_q as constants (combination 2) is

$$\boldsymbol{O}_{s2} = \begin{bmatrix} i_d R_s - L_d \dfrac{di_d}{dt} - \omega L_d i_q & -\omega^2 L_d \\ i_q R_s - L_q \dfrac{di_q}{dt} + \omega L_q i_d & R_s \omega \end{bmatrix} \tag{7}$$

The rows of $\boldsymbol{O}_{s2}$ correspond to second-order derivatives of i_d and i_q, respectively, and the columns represent the small variations in R_s and ψ_m. At steady state as long as $i_d \neq 0$ and $\omega \neq 0$ both R_s and ψ_m can be estimated. Only R_s is identifiable at $\omega = 0$. The columns of $\boldsymbol{O}_{s2}$ becomes linearly dependent when $i_d = 0$ that make it impossible to estimate R_s and ψ_m independently. Similar to the previous case, even when the average of i_d is zero while its derivative is not zero, both the parameters can be estimated simultaneously.

For the case of estimating L_d and ψ_m by keeping R_s and L_q as constants (combination 3), the proper sub matrix is

$$\boldsymbol{O}_{s3} = \begin{bmatrix} -2\dfrac{d^2 i_d}{dt^2} L_d + \omega\left(L_q \dfrac{di_q}{dt} - i_d L_d \omega\right) & -\omega^2 L_d \\ i_d R_s \omega & R_s \omega \end{bmatrix} \tag{8}$$

Similar to the previous combinations, the rows of $\boldsymbol{O}_{s3}$ correspond to second-order derivatives of i_d and i_q, respectively, but the columns represent small variations in L_d and ψ_m, respectively. The sub matrix $\boldsymbol{O}_{s3}$ is rank deficient even at steady state unlike the combinations 2 and 3. Therefore, the estimation of L_d and ψ_m is not at all possible unless there is a PE in the system.

The other possible two parameter combinations are L_q–ψ_m (combination 4), L_d–R_s (combination 5), and L_q–R_s (combination 6). The proper sub matrices of the combinations of 4 and 6 (not presented here) are full rank at steady state and even at $i_d = 0$. The combination 5 is fully observable at steady state as long as $i_d \neq 0$.

The rank analysis of the combinations of three and four parameters is presented in this paper by showing the proper sub matrix of four parameter combination, $\boldsymbol{O}_{s4}$. Each column corresponds to small variations in R_s, ψ_m, L_d, and L_q, respectively, and each row corresponds to first- and second-order derivatives of i_d and i_q, respectively. The columns corresponding to the parameters in a combination is only considered for finding the rank

$$\boldsymbol{O}_{s4} = \begin{bmatrix} -i_d & 0 & -\dfrac{di_d}{dt} & \omega i_q \\ -i_q & -\omega & -\omega i_d & -\dfrac{di_q}{dt} \\ [\boldsymbol{O}_{s3}] & & [\boldsymbol{O}_{s2}] & \end{bmatrix} \tag{9}$$

The sub matrices of three parameter combinations are rank deficient at steady state. The columns 3 and 4 together are linearly dependent with column 1 for combination 7 (L_d–L_q–R_s). For combinations 8 and 9 (L_d–L_q–ψ_m and L_d–R_s–ψ_m), the columns 3 and 4 are linearly dependent. The columns 2 and 4 together are linearly dependent with column 1 for the combination 10 (L_q–R_s–ψ_m). For combinations 9 and 10, the columns 1 and 2 are also linearly dependent at $i_d = 0$. The rank deficiency conditions of all of the three parameter combinations are also applicable to four parameter combination that make it rank deficient at steady state.

The summary of theoretical observability analysis with and without PE is presented in Table 1. The worst case operating states are compared, which include steady state, steady state and $i_d = 0$, and steady state and $\omega = 0$. The zero derivatives of i_d and i_q are defined as the steady state for the case without PE in this paper. No change in average of ripple currents over a span of sampling intervals is considered as steady state with PE. The estimation of both the parameters in some of the two parameter combinations at certain operating states without PE are rank deficient. The three and four parameter combinations are not at all observable at all the operating states without PE. These limitations on observability can be overcome with PE except in the case of $\omega = 0$. The parameter ψ_m is not identifiable at $\omega = 0$ and persistent current excitation cannot overcome this limitation.

All the theoretical results are validated for the reference IPM machine by simulation with the help of Matlab Simulink. The simulation without PE is carried out with field oriented control. The model predictive control (MPC) with finite control set (FCS) control is used for simulation with PE. It is shown that inherent high frequency vector injection in MPC with FCS is sufficient to create persistent current excitation. The simulation results are not included as this paper tries to validate most of the theoretical results by experiment.

3 Estimation scheme and experimental setup

The online estimation of different parameter combinations is realised by an RLS estimator. The RLS updates the error between actual (y) and estimated output ($\phi_n \theta_{n-1}$) to the next estimated parameters (θ_n) by a factor of Kalman gain. The Kalman gain is a function of covariance and forgetting factor. The forgetting factor decides the amount of contribution of the previous samples to the covariance. It plays a big role in the convergence accuracy and speed. Different forgetting factors are used for the different parameter combinations considered in this paper. The different combinations also have different mathematical formulations for the RLS estimator. The constant parameters and their coefficients in (4) move to be the part of the output. The varying parameters and their coefficients are formed as the product of measurement (ϕ) and the parameters (θ). For example, the mathematical formulation of RLS for combination 1 is

$$y_n = \phi_n \theta_{n-1} \tag{10}$$

where

$$\begin{gathered} y_n = \begin{bmatrix} v_{dn} - i_{dn} R_s \\ v_{qn} - i_{qn} R_s - \omega \psi_m \end{bmatrix}; \\ \phi_n = \begin{bmatrix} (i_{dn} - i_{d(n-1)})/T_s & \omega i_{qn} \\ (i_{qn} - i_{q(n-1)})/T_s & -\omega i_{dn} \end{bmatrix} \end{gathered} \tag{11}$$

In (11), v_{dn}, v_{qn}, i_{dn}, and i_{qn} stand for d- and q-axis voltages and currents, respectively, at current sampling interval (n). The variables $i_{d(n-1)}$, and $i_{q(n-1)}$ represent d- and q-axis currents of the previous sampling interval ($n-1$), and T_s is the sampling period. In this paper, the voltage samples are taken from the reference values and the currents are taken from the measurements.

$$\boldsymbol{O}_{s1} = \begin{bmatrix} -2\dfrac{d^2 id}{dt^2} L_d + \omega\left(L_q \dfrac{diq}{dt} - i_d L_d \omega\right) & i_q R_s \omega \\ i_d R_s \omega & -2\dfrac{d^2 iq}{dt^2} L_q + \omega\left(-L_d \dfrac{did}{dt} - L_q i_q \omega\right) \end{bmatrix} \tag{6}$$

Table 1 The summary of observability results with and without PE

Combinations	Steady state		Steady state + $i_d = 0$		Steady state + $\omega = 0$	
	Without PE	With PE	Without PE	With PE	Without PE	With PE
1, $L_d - L_q$	√	√	×	√	√	√
2, $R_s - \psi_m$	√	√	×	√	×	×
3, $L_d - \psi_m$	×	√	×	√	×	×
4, $L_q - \psi_m$	√	√	√	√	×	×
5, $L_d - R_s$	√	√	×	√	√	√
6, $L_q - R_s$	√	√	√	√	√	√
7–10, ${}^4C_3$	×	√	×	√	√[a]	√[a]
11, $L_d - L_q - R_s - \psi_m$	×	√	×	√	×	×

[a] For the combinations without parameter ψ_m

The software part of the experimental setup consists of mainly MPC with FCS and an RLS estimator. The MPC with FCS controls i_d and i_q in this work. The cost function is the error between the reference and predicted values of i_d and i_q. The prediction horizon is chosen as one. The MPC with FCS block in Fig. 1*a* outputs the voltage vector corresponding to the minimum cost function at each sampling time. The voltage vector is applied to electric machine via the inverter.

The experimental test bench consists of industrial grade IM and IPM machines configured back to back. The IM is driven by a Yokogawa motor drive. An in-house manufactured SiC inverter along with a DSpace Microautobox drives the IPM machine. The MPC with FCS scheme along with the RLS estimator is implemented in the Microautobox via Matlab Simulink. There are two encoders connected to each motor and six current feedback sensors to perform the field oriented control. A common DC bus (300 V) is used to supply both the machines. Fig. 1*b* shows the photo of the experimental setup. The control algorithm takes measurements and runs the estimation algorithm at the sampling rate of 10 kHz.

The reference IPM is a 5 kW, 1800 rpm machine with 28 Nm rated torque. The phase resistance at 25°C is 0.4 Ω and the no load permanent magnet flux linkage is 0.34 Wb. The nominal values of *d*- and *q*-axis inductances are 11 and 14.6 mH, respectively. The offline measured inductances for different i_d and i_q are shown in Fig. 2. The *q*-axis inductance decreases due to saturation as i_q increases and there is a considerable effect from cross saturation by i_d current. On the other hand, the *d*-axis inductance undergoes light cross saturation by i_q current.

4 Experimental results and discussions

The experiments are carried out to validate the theoretical observability results with PE presented in Section 2. The reason this paper focusing on PE is because, MPC-FCS which is being used always provides persistent current excitation even when the reference currents are zero. Furthermore, the different parameter combinations are different in terms of parameter observability, therefore, the experiments to estimate all the combinations are conducted even though some of them are not important in some practical cases.

4.1 Two parameter estimation

Combination 1 (L_d and L_q) is fully observable at steady state as long as $i_d \neq i_q \neq 0$ as mentioned in Section 2. However, the parameters are observable for the case of MPC-FCS even when the average $i_d = i_q = 0$ as shown in Fig. 3*a*. The small current ripples by vector injection are sufficient to make the system observable. The *d*- and *q*-axis current ripples are shown in Figs. 3*c* and *d*, respectively.

Combination 3 (L_d and ψ_m) is not observable at steady state and $i_d = 0$ without PE. The experimental results in Fig. 3*b* show that the current ripples (PE) associated with MPC-FCS are sufficient to overcome those limitations. The experiment is conducted when the average value of $i_d = 0$. The estimated parameters closely match with actual parameters.

The estimation of R_s and ψ_m (combination 2) is not observable at steady state when $i_d = 0$ without PE. The experimental results with MPC-FCS in Fig. 4*a* show that the system becomes observable for this case as there is a PE from current ripples. However, the parameters converge to wrong values with large oscillations especially for R_s. The current measurement noise and delays, and inverter non-linearities associated with the experiments are attributed to this behaviour. A small error in estimation of ψ_m results in a big error in R_s as they are tightly coupled by the *q*-axis machine equation (4). This behaviour would not be noticeable if the value of ψ_m was much lower than R_s by an order of one as verified by the simulation which is not presented here.

The coupling can be broken by keeping either $i_q = 0$ or $\omega = 0$. Fig. 4*b* shows the experimental results of estimating R_s and ψ_m with a very low speed ($\omega = 25$ rpm). The estimation is more

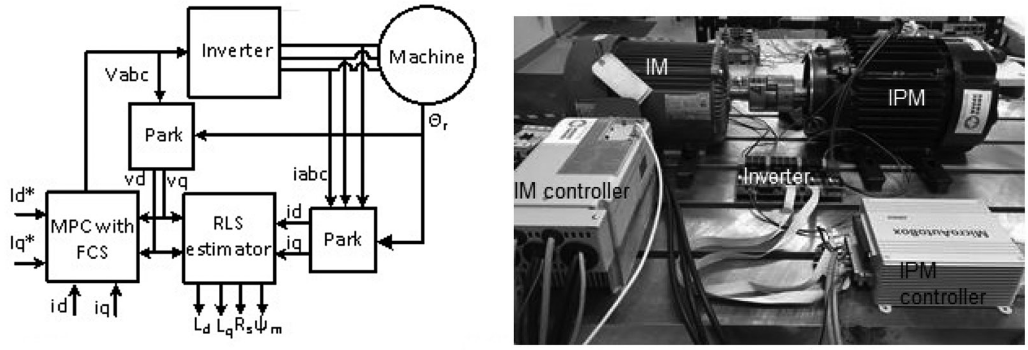

a *b*

Fig. 1 *Experimental scheme and setup*
a Block diagram of estimation with MPC with FCS
b Photo of experimental setup

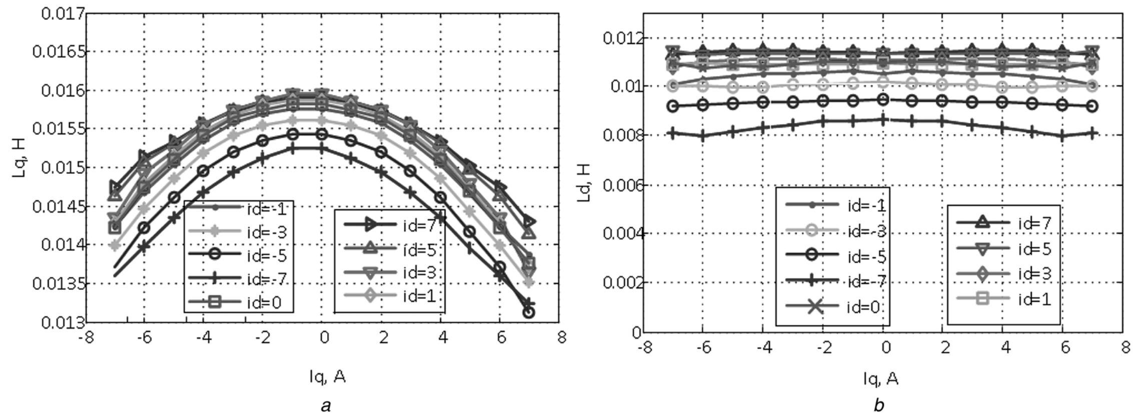

Fig. 2 *Offline measured inductances for different i_d and i_q*

a *q* axis inductance
b *d* axis inductance

accurate compared to Fig. 4*a*, however, there are still oscillations. This is due to the fact that, the complete decoupling is not made as ω is not exactly zero, which is not possible as long as estimating ψ_m. The complete decoupling can be achieved by keeping $i_q = 0$. The experimental results for the case with $i_q = 0$ are shown Fig. 4*c*. The parameters converged to the actual values. Decoupling by keeping $i_q = 0$ or $\omega = 0$ is not practically possible in the case of motor operation. Therefore, a decoupling technique is proposed in this paper.

4.2 Decoupling technique

A small variation in ψ_m creates a huge variation in R_s due to coupling. One way to overcome this coupling is to make the estimation of ψ_m insensitive to small variations by slowing down the convergence. It can be done by tuning the corresponding RLS forgetting factor. However, to get a reasonable steady estimation, the convergence is unreasonably slower.

The proposed decoupling technique in this paper separates estimation of R_s and ψ_m by two moderately fast RLSs (RLSs 1 and 2, respectively) as shown in Fig. 5*a*. The sampling rates of the two RLSs are kept high to avoid discretisation error due to low sampling rate (same as the main control algorithm, 10 kHz). The value of R_s updates to RLS 2 at each sampling time providing a direct link. On the other hand, RLS 2 starts the estimation of ψ_m with a prior known initial value. It updates to RLS 1 only when there is a considerable change (weak link). In this way, the small error in ψ_m estimation does not pass to R_s estimator while keeping the track of it.

The estimation of R_s and ψ_m (combination 2) is improved with decoupling technique as shown in Fig. 5*b*. The convergence of ψ_m is steady and accurate. There are still small oscillations in R_s. It can be further improved by tuning the RLS and the band of ψ_m

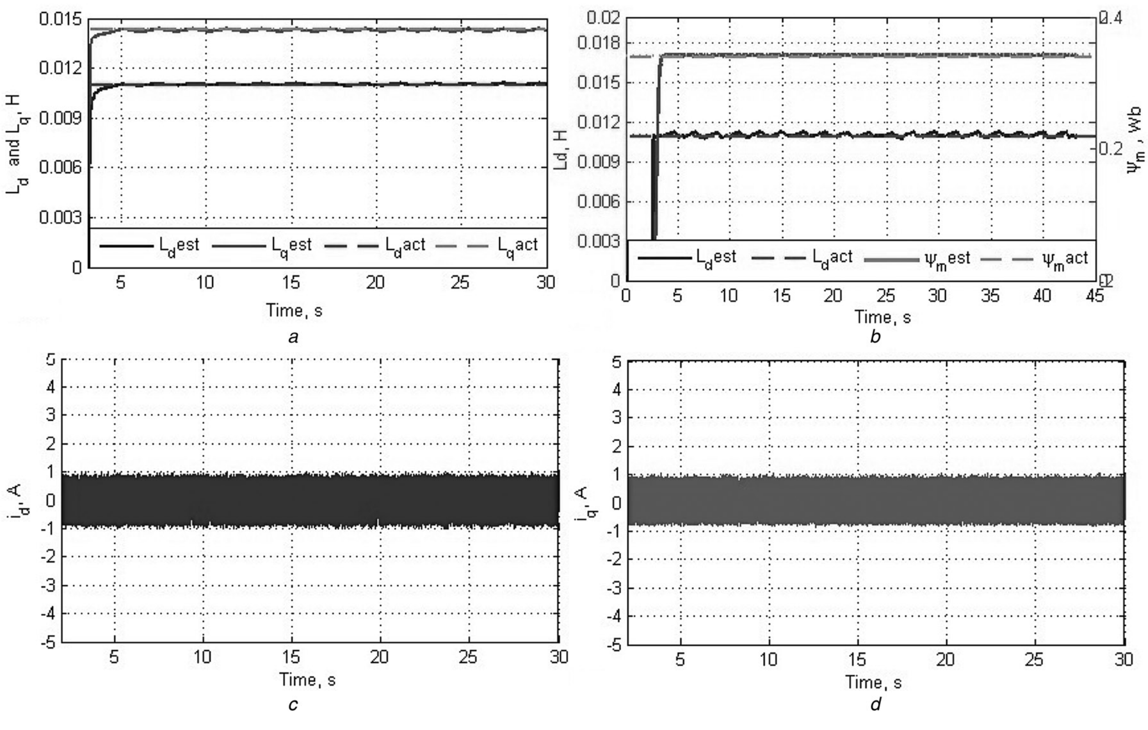

Fig. 3 *Experimental results*

a L_d–L_q estimation (combination 1)
b L_d–ψ_m estimation (combination 3)
c Average $i_d = 0$
d Average $i_q = 0$

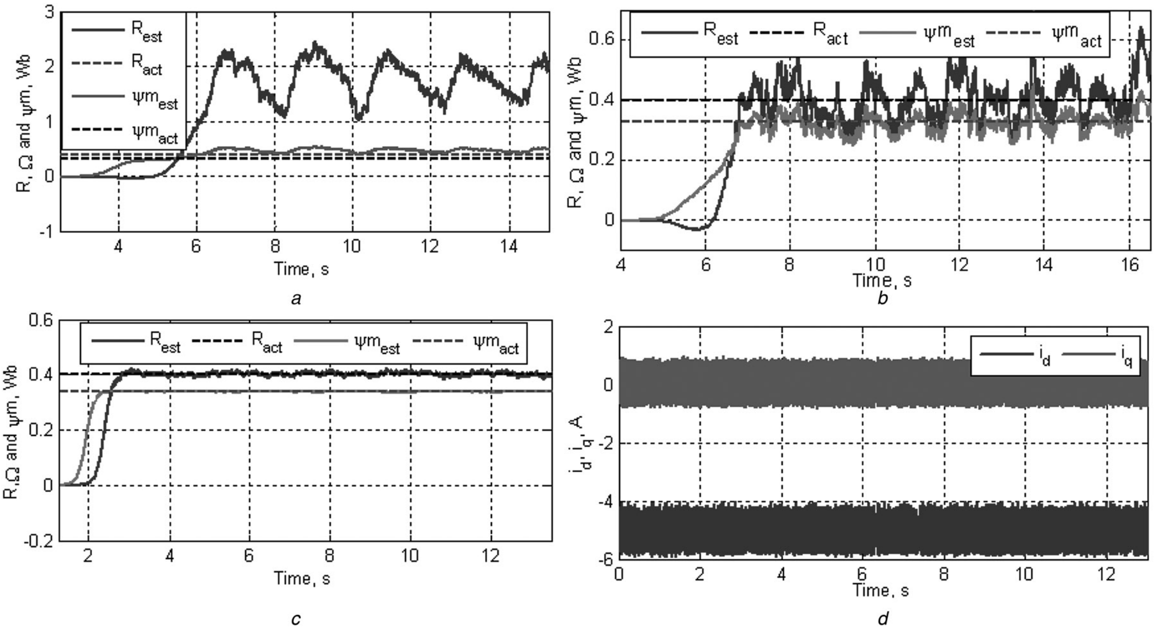

Fig. 4 *Experimental results of R_s and ψ_m estimation (combination 2)*

a For $i_q = 5$ A, $i_d = 0$ A, and 100 rpm
b For $i_q = 5$ A, $i_d = 0$ A, and 25 rpm
c For $i_q = 0$ A, $i_d = -5$ A, and 100 rpm
d Measured i_d and i_q for the case *c*

which decides whether to update RLS1 or not. Combination 2 only needs the decoupling among the two parameter combinations. The experimental results of combinations 4–6 are not presented in this paper as the convergence limitations are already demonstrated by the other three combinations.

4.3 Three parameter estimation

The three parameter combinations (7–10) are rank deficient at worst case operating states without PE as shown in Table 1. The parameter coupling also creates additional concern for some of the combinations. Combinations 7 and 8 do not need decoupling as R_s and ψ_m are not estimated simultaneously. The known constant values of R_s and ψ_m are provided, respectively, for combinations 7 and 8. The decoupling technique is applied for combinations 9 and 10. The parameter ψ_m is estimated separately by one RLS and the other two parameters are estimated by a second RLS.

The experimental results in Fig. 6 show that all the three parameter combinations converge to correct values with PE created by MPC with FCS. The average i_d is kept as zero in all the four cases (the worst case). There are small oscillations in R_s in combinations 9 and 10 which use decoupling technique similar to the case of combination 2. This can be improved by tuning RLS and band of ψ_m updater as mentioned before.

4.4 Four parameter estimation

The four parameter estimation with decoupling is realised by two RLSs. The first RLS estimates L_d, L_q, and R_s and the second one estimates ψ_m. The experiments are carried out at 50, 100, and 150 rpms. The i_q current is varied from 5 A with a step of 2 A until 11 A while keeping $i_d = 0$ A. The estimation results are shown in Fig. 7. The estimation of parameter ψ_m is steady and does not change with current and speed as expected. The parameter L_q decreases with increase in i_q due to saturation. The slight decrease in L_d is due to the cross saturation by i_q. Both L_d and L_q estimations follow the actual values. The parameter R_s is slightly over estimated at 50 rpm and becomes closer to the actual value at 100 rpm irrespective of the values of i_q. It is slightly under estimated at 150 rpm.

The experimental results show that the limitations on observability associated with all the parameter combinations can

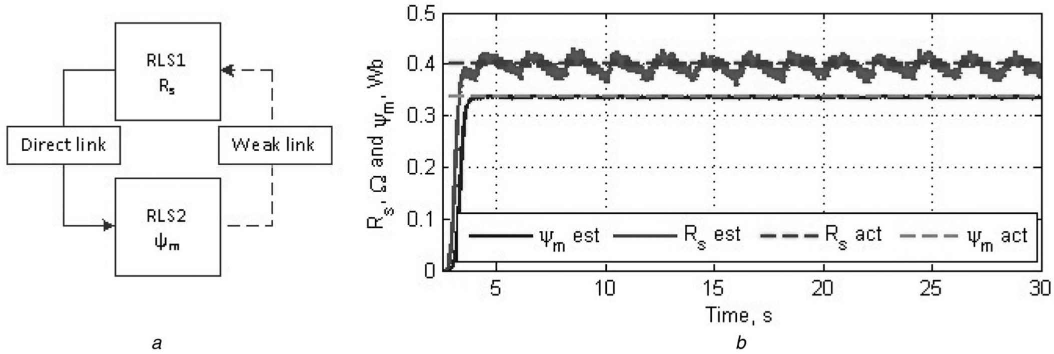

Fig. 5 *Decoupling technique*

a Two RLS configuration
b Experimental results of estimation R_s and ψ_m estimation (combination 2) at $i_q = 5$ A and 100 rpm

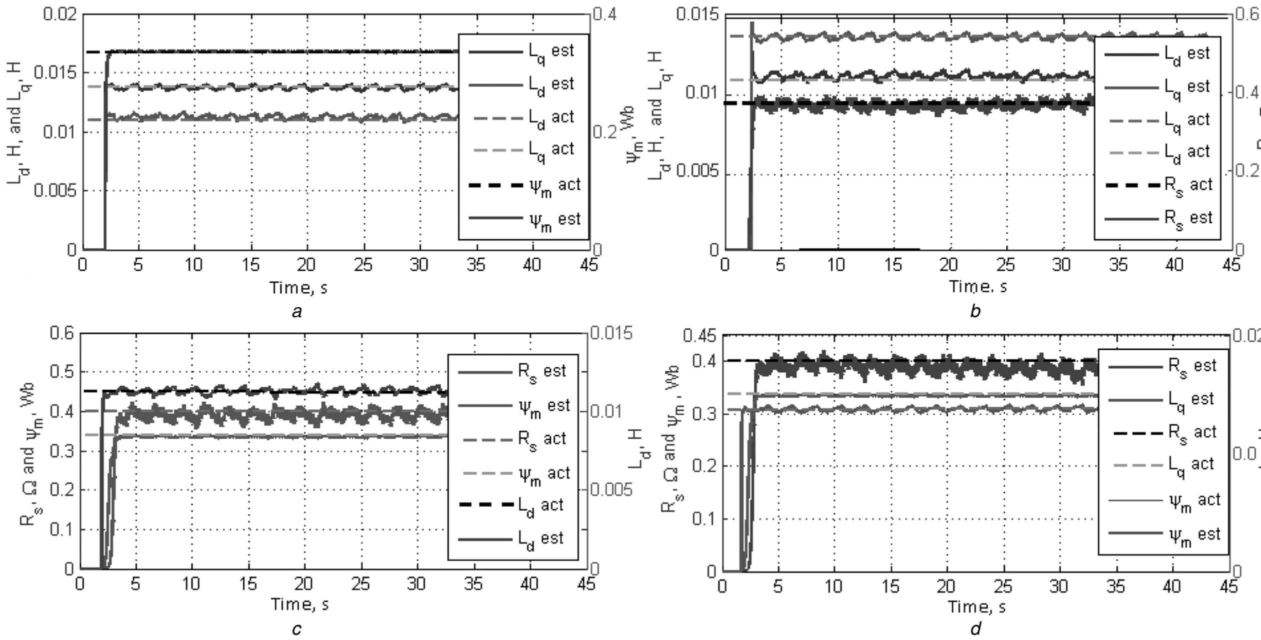

Fig. 6 *Experimental results of three parameter estimations at $i_q = 5\,A$, $i_d = 0\,A$, and 100 rpm*

a Combination 7 ($L_d - L_q - R_s$)
b Combination 8 ($L_d - L_q - \psi_m$)
c Combination 9 ($L_d - R_s - \psi_m$)
d Combination 10 ($L_q - R_s - \psi_m$)

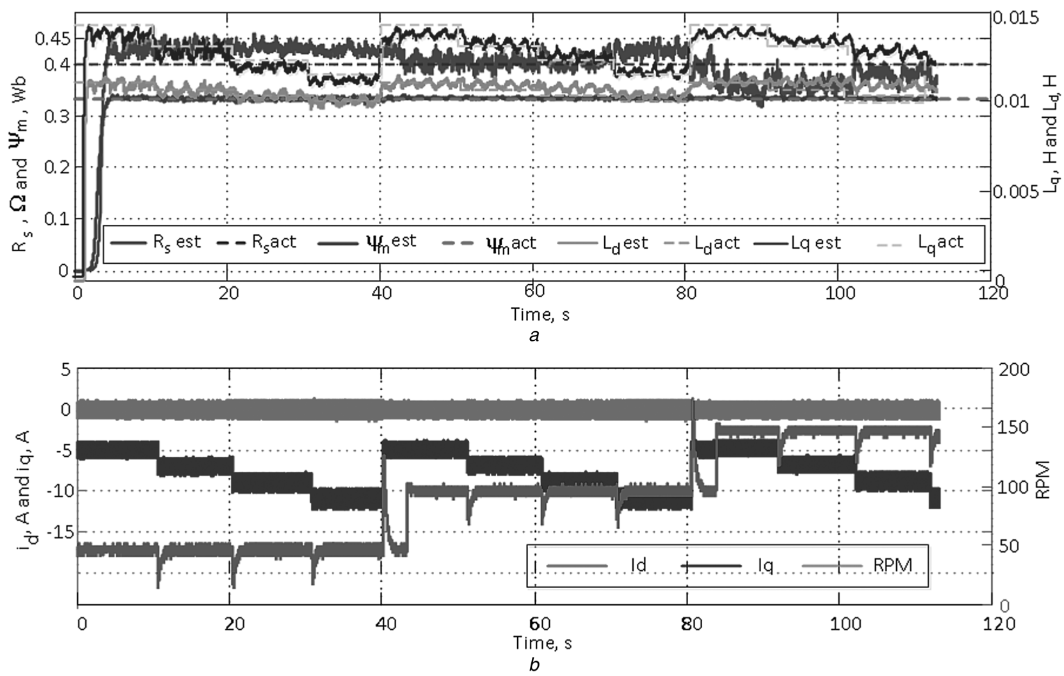

Fig. 7 *Experimental results*

a Estimation of combination 11 ($L_d - L_q - R_s - \psi_m$)
b Corresponding i_d, i_q and rpm

be overcome by persistent current excitation by MPC-FCS. So, one can choose any of the parameter combination based on the application as long as there is a PE. Not all the parameter combinations which are analysed in this paper have practical applicability. The four parameters are required to estimate for model-based control even though there is a position sensor. For example, the accuracy of torque prediction is dependent upon on the four parameters for direct torque control. MPC also needs the four parameters to accurately predict future control outputs. Similarly, all the four parameters are required for high speed sensorless control. The estimation of d- and q-axis inductances is required for accurately compensating cross coupling effects in linear control. The winding and magnet temperatures can be tracked by estimating winding resistance and permanent magnet flux linkage, respectively. Similarly, there are many more practical applications, however, this paper does not restrict the observability analysis to a certain application. It rather presents the observability in general for all of the parameter combinations.

5 Conclusion

This paper investigates the observability conditions to estimates the electrical parameters of an IPM machine with MPC-FCS. The observability of the system is different for different parameter combinations. This paper categorises the combinations into groups of two, three and four parameters. It is shown that some of the two parameter combinations are rank deficient without PE at steady state and $i_d = 0$ (the worst cases). All the three and four parameter combinations are rank deficient at the worst-case operating states. This paper proves experimentally that the current ripples created by inherent high frequency vector injection of MPC with FCS are sufficient to generate PE to overcome the limitations on observability. The parameter coupling which results in wrong convergence in estimation is analysed and a decoupling technique is proposed. Finally, the full parameter estimation with decoupling technique is validated experimentally at different operation points.

6 References

1 Emadi, A.: 'Advanced electric drive vehicles' (CRC Press, Boca Raton, FL, 2014), ISBN: 978-1-4665-9769-3

2 Xu, J., Wang, F., Xie, F., *et al.*: 'A new control method for permanent magnet synchronous machines with observer'. 2004 IEEE 35th Annual Power Electronics Specialists Conf., 2004, PESC 04, 2004, vol. 2, pp. 1404–1408

3 Li, M., Chiasson, J., Bodson, M., *et al.*: 'Observability of speed in an induction motor from stator currents and voltages'. Proc. 44th IEEE Conf. on Decision and Control, 2005, pp. 3438–3443

4 Kenne, G., Ahmed-Ali, T., Lamnabhi-Lagarrigue, F., *et al.*: 'Time-varying parameter identification of a class of nonlinear systems with application to online rotor resistance estimation of induction motors'. 2006 IEEE Int. Symp. on Industrial Electronics, Montreal, Que, 2006, pp. 301–306

5 Pavlov, A., Zaremba, A.: 'Adaptive observers for sensorless control of an induction motor'. Proc. of the 2001American Control Conf., 2001, Arlington, VA, 2001, vol. 2, pp. 1557–1562

6 Del Vecchio, D., Murray, R.M.: 'Observability and local observer construction for unknown parameters in linearly and nonlinearly parameterized systems'. Proc. 2003American Control Conf., 2003, 2003, vol. 6, pp. 4748–4753

7 Basic, D., Malrait, F., Rouchon, P.: 'Euler-Lagrange models with complex currents of three-phase electrical machines and observability issues', *IEEE Trans. Autom. Control*, 2010, **55**, (1), pp. 212–217

8 Laroche, E., Sedda, E., Durieu, C.: 'Methodological insights for online estimation of induction motor parameters', *IEEE Trans. Control Syst. Technol.*, 2008, **16**, (5), pp. 1021–1028

9 De La Guerra, A., Maya-Ortiz, P., Espinosa-Pérez, G.: 'Global observability analysis of the SR Motor under sensorless operation'. 2015 54th IEEE Conf. on Decision and Control (CDC), Osaka, 2015, pp. 1799–1804

10 Sontag, E.D.: 'A concept of local observability', *Syst. Control Lett.*, 1984, **5**, pp. 41–47, North-Holland October 1984

11 Hermann, R., Krener, A.: 'Nonlinear controllability and observability', *IEEE Trans. Autom. Control*, 1977, **22**, (5), pp. 728–740

12 Boileau, T., Leboeuf, N., Nahid-Mobarakeh, B., *et al.*: 'Online identification of PMSM parameters: parameter identifiability and estimator comparative study', *IEEE Trans. Ind. Appl.*, 2011, **47**, (4), pp. 1944–1957

13 Vaclavek, P., Blaha, P., Herman, I.: 'AC drive observability analysis', *IEEE Trans. Ind. Electron.*, 2013, **60**, (8), pp. 3047–3059

14 Zaltni, D., Abdelkrim, M.N., Ghanes, M., *et al.*: 'Observability analysis of PMSM'. Third Int. Conf. on Signals, Circuits and Systems (SCS), 2009, Medenine, 2009, pp. 1–6

15 Liu, Q., Hameyer, K.: 'A fast online full parameter estimation of a PMSM with sinusoidal signal injection'. 2015 IEEE Energy Conversion Congress and Exposition (ECCE), Montreal, QC, 2015, pp. 4091–4096

16 Underwood, S.J., Husain, I.: 'Online parameter estimation and adaptive control of permanent-magnet synchronous machines', *IEEE Trans. Ind. Electron.*, 2010, **57**, (7), pp. 2435–2443

17 Xu, W., Lorenz, R.D.: 'High-frequency injection-based stator flux linkage and torque estimation for DB-DTFC implementation on IPMSMs considering cross-saturation effects', *IEEE Trans. Ind. Appl.*, 2014, **50**, (6), pp. 3805–3815

18 Dang, D.Q., Rafaq, M.S., Choi, H.H., *et al.*: 'Online parameter estimation technique for adaptive control applications of interior PM synchronous motor drives', *IEEE Trans. Ind. Electron.*, 2016, **63**, (3), pp. 1438–1449

19 Kallio, S., Karttunen, J., Peltoniemi, P., *et al.*: 'Online estimation of double-star IPM machine parameters using RLS algorithm', *IEEE Trans. Ind. Electron.*, 2014, **61**, (9), pp. 4519–4530

20 Preindl, M., Bolognani, S.: 'Model predictive direct speed control with finite control set of PMSM drive systems', *IEEE Trans. Power Electron.*, 2013, **28**, (2), pp. 1007–1015

21 Preindl, M., Bolognani, S.: 'Model predictive direct torque control with finite control set for PMSM drive systems, part 1: maximum torque per ampere operation', *IEEE Trans. Ind. Inform.*, 2013, **9**, (4), pp. 1912–1921